ARTICLES

Excitation and Emission Properties of Platinum(II) Acetylides at High and Low Concentrations

Eirik Glimsdal,*,† Patrick Norman,*,‡ and Mikael Lindgren*,†

Department of Physics, Norwegian University of Science and Technology (NTNU), NO-7491 Trondheim, Norway, and Department of Physics, Chemistry and Biology, Linköping University, SE-581 83 Linköping, Sweden

Received: June 10, 2009; Revised Manuscript Received: August 28, 2009

Photophysical properties of platinum(II) acetylides in tetrahydrofuran (THF) solutions and incorporated in poly(methyl methacrylate) (PMMA) glasses have been studied over a large concentration range from 10 μM to 50 mM. In general, the luminescence properties of the studied chromophores in the liquid state were also maintained in the solid state, except for shorter decay times of 50−90 μs of the triplet state in the glass compared with 200−300 μs in solution at low concentrations. The phosphorescence line shapes were found to be independent of both the chromophore concentration and the environment (THF and PMMA). The triplet state lifetimes did not change with concentration in the solid-state case, whereas, in solution, the decay becomes shorter at increasing concentration. The latter effect could be modeled with an additional linear quenching rate, k_q, in the range of (1 to 7) $\times$ 10^7 M^{-1} s^{-1}. Excitation spectra of the triplet state at high concentrations, in both solutions and solid glasses, showed additional excitation bands on the long wavelength side compared with the corresponding measurements at low concentrations. This indicates enhanced singlet−triplet coupling due to intermolecular electronic interactions that become important at concentrations of 0.1 to 1 mM and above.

Introduction

Lasers are becoming widely used in electronic devices and instruments in many applications as new and powerful lasers operating at a variety of different wavelengths are being developed.[1] High-power lasers can efficiently be used to destroy optical sensors, including the eye.[2] Therefore, the demand for optical sensor protection devices against powerful light has increased. A suitable eye protective device needs to function at all wavelengths in the visible region and at different pulse energies, pulse lengths, and pulse repetition frequencies (prf's).[3] Protection can be achieved by utilizing the self-activating nonlinear optical (NLO) properties of different materials,[4] a process often referred to as optical power limiting (OPL). OPL materials should have high transmission for low-intensity light and a successive reduction in the transmitted power at higher intensities so that no damage occurs in the protected sensor.[5]

The photophysical mechanisms utilized for OPL in NLO materials are based on two-photon absorption (TPA), excited state absorption (ESA), nonlinear refraction, and optically induced scattering.[5,6] TPA may give a strong nonlinear response for short high-amplitude pulses, whereas ESA from long-lived triplet states may give the desired properties over longer pulse lengths.[7] Platinum(II) acetylides in monomer[8] and polymer[9] form have been widely investigated for their photophysical and structural properties[10] for use in OPL devices.[11] The chromophores have been found to have special characteristic capabilities suitable for strong nonlinear absorption of high-intensity radiation in the visible region, whereas they maintain their good optical transparency for low-intensity light of the same wavelengths.[12]

In a recent study, a selection of Pt−acetylide molecules was incorporated into solid PMMA matrices for the development of a solid-state OPL device.[13,14] In one type of glass material, the chromophores Z1, Z3, and Pt1 (Figure 1) were dispersed in MMA before polymerization (type I glass). For the purpose of improving the stability performance, a second approach was also investigated. Here the Pt1 chromophore was functionalized to covalently bond to the solid PMMA matrix during the polymerization process (Pt1−methacrylate in Figure 1) to constitute a type II glass. (See Westlund et al.[14] for more details.) Raman spectra of the doped solid devices proved that the chemical structure of the nonlinear dyes remains intact upon the polymerization of the solid matrix,[14] and basic luminescence spectra confirm that the basic photophysical properties observed for the solute molecules in tetrahydrofuran (THF) solutions are also maintained in the solid state for both type I and type II PMMA glasses.

In this study, we examined the three Pt(II)−acetylides (1) in solid PMMA and determined their photophysical properties at both low and high doping levels, where the latter has the potential to be used as an OPL device. The results from low and high concentration measurements in solid PMMA are compared with similar concentration measurements with the chromophores in liquid THF solutions. Spectral assignments were made with the aid of first principles time-dependent density

* Corresponding author.
† Norwegian University of Science and Technology.
‡ Linköping University.

10.1021/jp905437c CCC: $40.75
Published on Web 09/28/2009

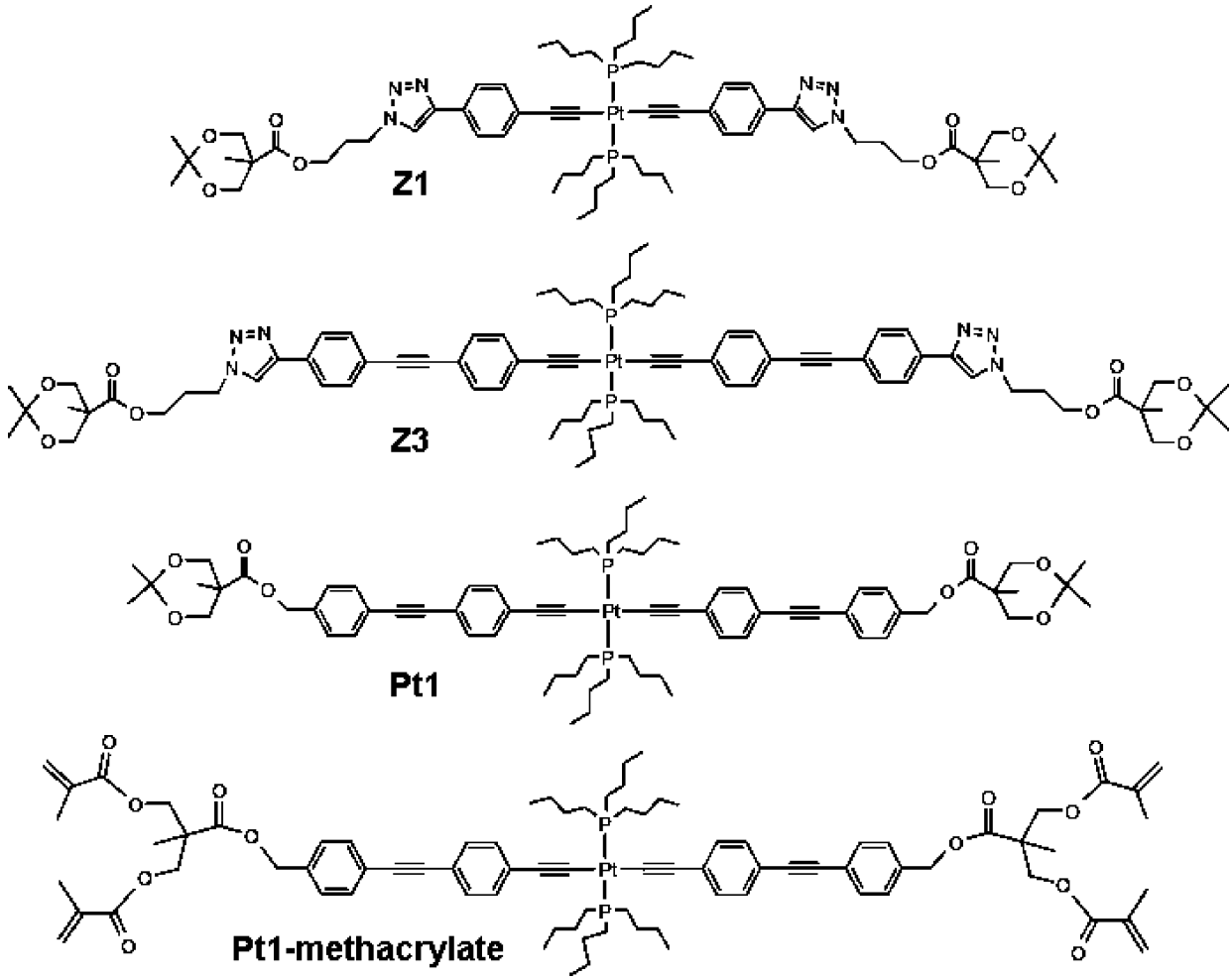

Figure 1. Molecular structures of Z1, Z3, and Pt1 used in liquid samples and in type I PMMA glass and Pt1−methacrylate for covalent bonding in type II PMMA glass.

functional theory (TD-DFT) calculations. From these calculations, we determined ground-to-excited and excited-to-excited state transition energies and oscillator strengths. At our level of theory, oscillator strengths are zero for transitions that do not conserve spin symmetry, and in these cases only the transition energies are reported. All TD-DFT calculations were performed with the ground state as the reference state; the linear absorption properties for the ground-to-excited state transitions are retrieved from the first-order residue of the linear response function, whereas the same properties for the excited-to-excited state transitions are retrieved from the second-order residue of the quadratic response function. This is an approach that has been implemented for most standard electronic structure methods, and a presentation of the details of the general approach is found in, for example, the review of Norman and Ruud.[15]

Methods

Experimental Details. Samples between 0.01 and 50 mM concentration could be made using MMA both for further polymerization into solids and for comparison with THF solutions. Absorption and luminescence measurements for solution samples were performed using a 10 mm quartz cell (Hellma Precision) possible to attach to a vacuum line for air evacuation. Because the latter samples required 3 to 4 mL volume, it was possible to reach only ∼5 mM concentration in these experiments with the materials available. Similar spectroscopic measurements were performed on 1.5 mm thick doped PMMA glasses of 1 cm diameter at concentrations from 10 μM up to 50 mM prepared as described in a previous study.[14] As for the transient absorption measurements, a 1.5 mm path 50 mM solid sample has a comparable linear transmission to that of a 5 mM 10 mm path liquid sample. Steady-state optical absorption and transmission measurements were recorded using a Shimadzu UV-1601PC spectrometer. Luminescence spectra and excited-state decay times were recorded using a Jobin Yvon IBH FluoroCube photon-counting spectrometer. For more details of the overall setup, see Glimsdal et al.[16]

Both the IBH NanoLED excitation source at 337 nm, with a prf of 1 MHz and 1.1 ns pulse length, and the white flashlamp at 20 Hz, with <1 μs pulse length, were used as excitation sources depending on the experiment. We recorded steady-state emission by scanning the monochromator in front of the PMT for a given prf and fixed excitation wavelength. We recorded excitation spectra in a similar way by scanning the monochromator at the flashlamp side at a fixed emission monitoring wavelength. Phosphorescence decay times were measured using the system in multichannel scaling (MCS) mode, with the highest time resolution of 500 ns per channel, in a typical time range of 1000 channels.

A flash photolysis equipment, as described by Glimsdal et al.,[17] composed of commercial and purpose-built units, was used in the triplet ESA measurements. The pump flash of ∼5 μs duration triggers the probe lamp (with a duration of ∼2 μs) after a variable preset delay, typically 5−10 μs. A detailed

description of the method, setup, and instruments is found in Glimsdal et al.[17] The limiting time resolution of the system is determined by the temporal width of the probe flash. Solid-state samples were placed at 45° to both pump and probe light in the experimental setup to avoid direct scattering into the detector.

Computational Details. In the theoretical work, the molecular structures are those of the basic molecules Pt1, Z1, and Z3 in Figure 1 but without the bis-MPA units and with the use of methyl-terminated phosphine ligands. All calculations refer to isolated molecules and were performed at the nonrelativistic level of theory but with relativistic effective core potentials from the Stuttgart group for platinum[18] and phosphorus.[19] Molecular structure optimizations of the singlet ground state and the lowest triplet excited state were performed at the restricted and unrestricted Kohn−Sham level of theory, respectively, and using the B3LYP exchange-correlation functional[20] and a polarized 6-31G* basis set for C and N and a 6-31G basis set for H.[21]

The response calculations utilize, in addition to the parametrization described above, the Coulomb attenuated method B3LYP (CAM-B3LYP) functional[22,23] and the improved augmented correlation consistent basis sets of Dunning (aug-cc-pVDZ).[24] Calculations with the B3LYP functional were carried out with the Gaussian program,[25] whereas those with the CAM-B3LYP functional were carried out with the Dalton program.[26]

Results and Discussion

Ground-State Linear Absorption and Transmission. ***Molecular Conformations.*** The three molecules Pt1, Z1, and Z3, all have a ground state of singlet spin symmetry with a large energy gap of 5 to 6 eV between occupied and unoccupied electronic states at the DFT/CAM-B3LYP level of theory, and the delocalized and π-conjugated frontier orbitals determine the optical properties of the compounds. The molecular structures were optimized for all molecules in their respective ground singlet (S_0) and first excited (T_1) electronic states without enforcing any point group symmetry. A vibrational analysis was performed in all cases for the resulting configurations to ensure that the corresponding Hessian matrices are positive definite. The rotational barrier for C−Pt−C bond rotation is obviously small in the studied systems. Molecular structures where the phenyl rings lie in the plane of the P−Pt−P center will be referred to as planar. A situation where the phenyl ligands are rotated by 90° is referred to as a twisted conformation.

The molecular structure optimizations were performed with initial configurations that had small asymmetric bond twists of about 5° with respect to the planar structures. Given these initial structures, Pt1, Z1, and Z3 returned to planar ground-state optimized configurations with a number of bond lengths in common: a Pt−C bond length of 2.02 Å, carbon triple bond lengths of 1.23/1.22 Å, and carbon−phenyl bond lengths of 1.43/1.42 Å (where the report of two bond lengths refers to the first and second alkyne group in the ligands of Pt1 and Z3, respectively). We carried out optimizations of the triplet state in the same manner; also, in these cases, all three molecules were predicted to be planar. In addition to a plane, the ground state (but not the excited state) of Pt1 also has a C_2 rotation axis perpendicular to the molecular plane as a symmetry element. A correct nonrelativistic labeling of the planar ground state of Pt1 is therefore X^1A_g (C_{2h} point group), whereas the planar ground states of Z1 and Z3 are denoted as X^1A' (C_s point group); the planar triplet states are for all three molecules denoted as $1^3A'$ (C_s point group).

There is, however, reason to believe that the prediction of planar ground state structures for the smaller molecules may be due to steric interactions between the phenyl and the methyl groups that provide a small rotational barrier. To investigate this issue of twisted configurations, we also performed structure optimizations for Pt1 with initial structures that had close to 90° twisted ligands. The ground and excited states both remain in twisted configurations upon optimization. It is seen that for the ground state the twisted configuration is 36 meV lower in energy than the corresponding planar configuration, whereas the opposite was found for the triplet state, with an energy difference of 44 meV. It is clear that the potential energy surfaces with respect to these C−Pt−C bond twists are very flat, and rotations will occur in the liquid phase at room temperature.

Spin-Allowed Transitions. The ground-state linear absorption spectra are strongly dominated by transitions induced by an electric field polarized along the molecular conjugation axis, and, in the visible region, the (by far) most intense transition is to the lowest excited state, S_1. For the respective molecules, we report in Table 1 vertical electronic excitation energies and oscillator strengths for the $S_0 \rightarrow S_1$ transition. The results obtained with the use of the B3LYP functional do suffer from the by now well-known problem of an incorrect asymptotic limit of the electron−hole Coulomb interaction, which inflicts underestimated excitation energies. A remedy for this deficiency in the functional is the Coulomb attenuating method that, with respect to charge separation, gradually increases the amount of exchange interactions in the functional. As a part of this strategy, the CAM-B3LYP functional has been developed[22] and, when benchmarked against wave function correlated methods, has also proven to be quite accurate, even for nonlinear response properties that are very sensitive to the treatment of electron correlation.[27] From the results presented in Table 1, we note that the discrepancy in singlet-state transition energies amounts to about 0.6 to 0.7 eV; we here compare B3LYP/6-31G* and CAM-B3LYP/6-31G results. (Because the influence of the polarization functions is expected to be small, this comparison is an appropriate one.) With an improved basis set (aug-cc-pVDZ), the transition energies are reduced by about 0.15 eV as a consequence of an improved description of the more diffuse excited state. We believe the CAM-B3LYP/aug-cc-pVDZ approach to be state-of-the-art for the optical properties considered here, and we include the less accurate results merely to illustrate the sensitiveness with respect to the basis set and the long-range Coulomb interaction.

The ground-state absorption peaks are predicted to fall outside the visible region at transition wavelengths of 332 (3.73 eV), 355 (3.49 eV), and 365 nm (3.40 eV) for Z1, Pt1, and Z3, respectively, and with increasing integrated absorption cross sections in that order. For Pt1, we have also determined the ground-state absorption in the twisted conformation (footnote d of Table 1), and the energy gap is seen to increase by 0.31 eV upon symmetric rotation of the ligands. It is clear that in reality the absorption spectrum is to be understood as an average over all possible ligand conformations (for which rotation is virtually free at room temperature) and that our considering only two of these is a severe restriction. However, our limited calculation does indicate that if such an averaging were carried out, then one would predict a broadened absorption band due to the variations in $S_0 \rightarrow S_1$ transition energies and oscillator strengths. In Figure 2, we show the experimental transmission spectra of Z3 and Pt1 dissolved in THF (panel A) as well as embedded in PMMA glass (panel B). We note that transmission spectra for low dye concentrations have previously been

TABLE 1: Electronic Energies (electronvolts) and Oscillator Strengths for the Excited Singlet (S_1) and Triplet States (T_1 and T_n)[a]

			S_1		T_1			T_1[b]	
molecule	method	basis[c]	ΔE_v	f	ΔE_v	ΔE_{0-0}	ΔE_p	ΔE_v	f
Pt1[d]	ΔB3LYP	B			2.73	2.25	1.92		
	TD-B3LYP	B	2.99	2.46	2.23		1.65		
	TD-CAMB3LYP	A	3.65	3.01	2.30		1.53	2.69	0.38
		C	3.49	3.16	2.21		1.44	2.66	1.01
Pt1[e]	ΔB3LYP	B			3.06	2.33	1.98		
	TD-B3LYP	B	3.41	2.67	2.36		1.69		
	TD-CAMB3LYP	A	4.03	3.82	2.38		1.54	2.67	0.37
		C	3.80	3.72	2.29		1.45	2.64	0.75
Z1[d]	ΔB3LYP	B			2.91	2.69	2.49		
	TD-B3LYP	B	3.26	1.47	2.49		2.13		
	TD-CAMB3LYP	A	3.87	1.65	2.58		2.18	2.72	2.58
		C	3.73	1.79	2.49		2.09	2.64	1.18
Z3[d]	ΔB3LYP	B			2.71	2.19	1.86		
	TD-B3LYP	B	2.88	3.07	2.16		1.59		
	TD-CAMB3LYP	A	3.56	3.89	2.23		1.49	2.92	2.43
		C	3.40	4.05	2.14		1.39	2.74	3.65

[a] Subscripts v, p, and 0−0 refer to vertical absorption, phosphorescence, and minima separation of electronic energies, respectively. Data for S_1 and T_1 are reported with reference to the ground state (S_0), whereas data for T_n is given with respect to T_1. [b] Refers to the dominating $T_1 \rightarrow T_n$ transition in the visible region. [c] Results are obtained with basis set 6-31G for H, the Stuttgart ECPs for Pt and P, and basis sets (A) 6-31G, (B) 6-31G*, and (C) aug-cc-pVDZ for C and N. [d] Planar molecular structure in S_0 and T_1 states. [e] Molecular structure with 90° rotatation of ligands in S_0 and T_1 states.

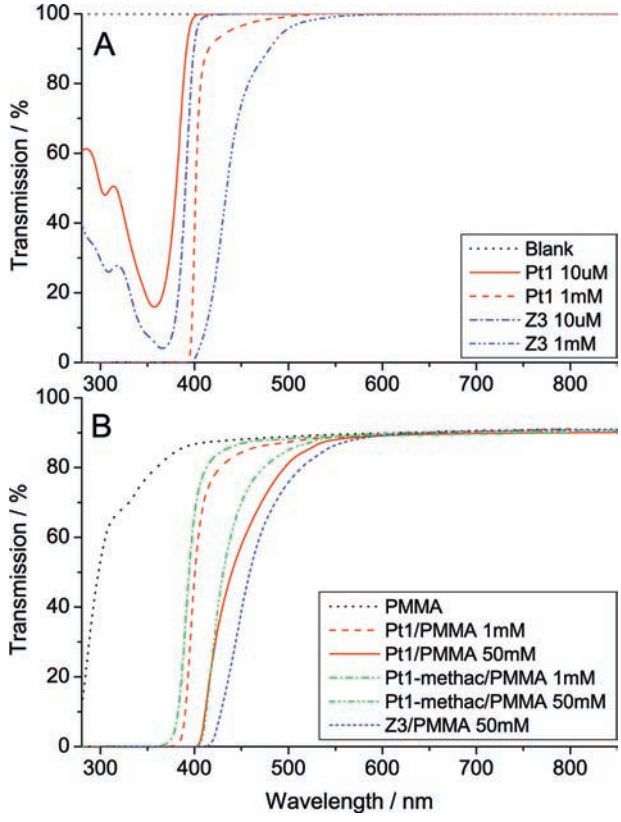

Figure 2. Transmission spectra of (A) Pt1 and Z3 in THF solution and (B) Pt1, Pt1-methacrylate, and Z3 in PMMA glasses.

reported,[13,14] but, for completeness, these are also reported here together with the corresponding high-concentration spectra. In solution at low dye concentrations, the Z3 and Pt1 samples are seen to be virtually transparent for wavelengths larger than 400 nm. The transition edge from transparent to opaque for Z3 and Pt1 occurs at wavelengths around 390 and 380 nm, respectively. The absorption maximum found from experiment are reported to be 342 (Z1), 357 (Pt1), and 365 nm (Z3),[13,28] and it is clear that our theoretical results, obtained from a single optimized molecular conformation, compare well with these experimental λ_{max} results.

As the concentration increases, the tail of the absorption bands naturally raises, resulting in considerable absorption below approximately 500 and 530 nm at a 1 mM concentration for Pt1 and Z3, respectively. We will discuss in more detail the issue of concentration-dependent absorption characteristics in the subsequent section in connection with spin-forbidden transitions.

In the PMMA case, which is shown in Figure 2B, a similar trend is observed. Here the background PMMA contribution has not been corrected for to better resemble the absorption properties of a real OPL device. At the lowest concentrations (10−100 μM), the absorption band starts at ∼400 nm, just as in the liquid case. At higher concentrations, the absorption in the 400−550 nm region increases, and at 50 mM, the transmission becomes clearly reduced below 520 and 550 nm for Pt1−methacrylate/PMMA and Pt1/Z3/PMMA, respectively. This absorption is responsible for a yellow coloring of the high-concentration samples. However, the visibility through the samples is still very good at high concentrations.

Spin-Forbidden Transitions. The theoretical transition wavelengths for vertical absorption to the lowest triplet states are 498 (2.49 eV), 561 (2.21 eV), and 579 nm (2.14 eV) for Z1, Pt1, and Z3, respectively. Experimentally, however, we record, not the direct absorption from S_0 to T_n but instead the phosphorescence emission that follows pumping of the S_1 state. The population of the triplet states occurs then only after an intersystem crossing from S_1 to the triplet manifold, and this crossing has the highest yield for triplet states that are nearly degenerate with S_1 (which in the present cases are states T_2 and T_3). The time scale of the nonradiative vibronic relaxation within the triplet manifold therefore becomes an issue in the comparison between theoretical and experimental data and so does the conformational averaging. If a complete relaxation to the lowest vibrational state of T_1 was to occur before light emission, the relevant transition energies to compare with would be those denoted as ΔE_p in Table 1. Given the several low-

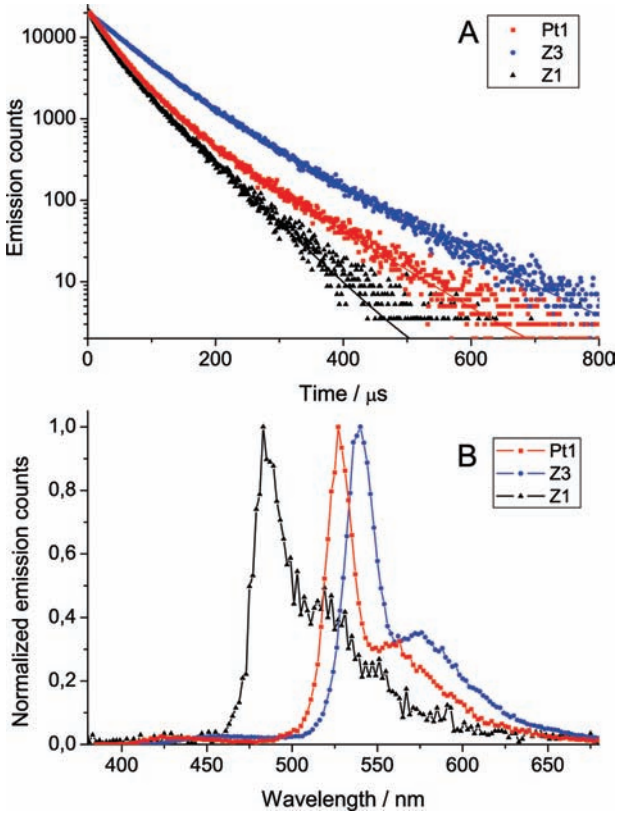

Figure 3. (A) Phosphorescence time decay trace and (B) emission spectra of Z1, Z3, and Pt1 in PMMA (type I) at a dye concentration of 50 mM. The emission decays were obtained at the respective emission peak and with excitation pulses at 360 nm. The decay time and emission spectrum of Pt1 in type II glass are essentially identical as for type I (data not shown).

energy vibrational modes in the considered systems, such a complete relaxation will not occur at room temperature, and, as discussed above, the ligands will be more or less freely rotating. We therefore expect large broadenings in the experimental spectra, which will prohibit quantitative comparisons between theory and experiment. But we note that the experimental emission peaks in the lower panel of Figure 3 occur at wavelengths of 485, 530, and 540 nm for Z1, Z3, and Pt1, respectively, which thus at least give credit to the theoretical description of the triplet manifold.

The reported emission spectra in Figure 3 are obtained for PMMA embedded chromophores of type I glass, but they are in agreement with the corresponding spectra obtained in THF solution.[28] Emission decay traces measured at the emission peaks are shown in Figure 3A. It is interesting to note that the decay traces are not single exponentials. However, an analysis based on two components could be used to fit the experimental decay data. For the PMMA glasses with dye concentrations of 50 mM, this analysis of the decay traces provided the following decay times and amplitudes of the total decay trace; Z1: 24 μs (36%), 58 μs (64%); Z3: 60 μs (67%), 113 μs (33%); and Pt1: 36 μs (66%), 90 μs (34%). Because the two components of the decay were found to be of similar magnitude, it cannot be ascertained that a two-component model is valid or that an even more complex model should be used.[29] From the parameters obtained from the two-component model, we may determine an average decay time according to

$$\bar{\tau} = f_1\tau_1 + f_2\tau_2 \quad \text{with} \quad f_i = \frac{\alpha_i\tau_i}{\sum_j \alpha_j\tau_j} \tag{1}$$

where α_i and τ_i are the amplitude and lifetime of the two separate exponential decay channels[29] because such a parameter is useful for comparing different samples. The calculated average lifetimes are given in Table 2. The decay times of Z3 and Pt1 in PMMA are shorter than those found in low-concentration oxygen-evacuated solution. The considerable shorter decay time of Z1 in solution (see below) suggests that other efficient quenching mechanisms are in operation for this molecule. No particular changes in the decay traces were found at lower chromophore concentrations in PMMA. Both the emission spectrum and the emission decay trace were found to be essentially identical for Pt1 and Pt1−methacrylate in PMMA.

Concentration Dependence of Triplet State Excitation and Emission Spectra. ***Phosphorescence Decay Rates.*** In solution, the emission spectra of Pt1, Z1, and Z3 exhibit only weak fluorescence around 400 nm with quantum efficiencies on the order of 10^{-3} and even weaker phosphorescence bands at 490 nm for Z1 and around 530−540 nm for Pt1 and Z3.[13,28] After air evacuation, the phosphorescence peaks recorded in THF solution were greatly enhanced for Pt1 and Z3 with peaks at 527 and 538 nm for Pt1 and Z3, respectively (corresponding to two of the peaks in PMMA in the lower panel of Figure 3), and the position and shape of the emission peaks were found to be the same for all concentrations. The corresponding phosphorescence decay times in 10 μM solutions increased by 3 orders of magnitude from 260 ns to 190 μs for Pt1 and from 260 ns to between 250 and 310 μs for Z3. In contrast, the phosphorescence emission spectrum and decay time of Z1 was increased by only one order of magnitude from 50 ns to 0.6 μs after air evacuation. Because of the weak phosphorescent signal, it was not possible to establish the concentration dependence in this case.

In contrast with the case of dyes dissolved in PMMA, all decay spectra of solution samples were found to be pure single exponential in character, and at higher concentrations, the observed phosphorescence decay times were found to be shorter. For Pt1, the decay times were 190 μs for 10 μM, 170 μs for 100 μM, 100 μs for 500 μM, and 54 μs for 1 mM. For the Z3 compound, the decay traces and lifetimes are shown in Figure 4A and are further discussed below.

Quenching of Triplet States in Solution. The quantum efficiency of the phosphorescence emission channel is estimated to be approximately 4−6% after air evacuation in 1−10 μM solutions. The reduced decay times at higher concentrations are accompanied by reductions of the phosphorescence yield in the experiment. Because the electric−dipole coupling between the ground state and the triplet state is increasing with higher concentrations (as will be discussed in the subsequent section), the reduced phosphorescence quantum yields must be due to a more strongly increased probability for triplet state quenching in high concentrations. Similar observations have previously been made for excimer formation of a Pt-based molecule in the liquid phase.[30]

The reduced decay times were fitted to a linear model of concentration-dependent triplet quenching. In this model, the observed decay rate ($k = 1/\tau$) is the sum of the decay rate in the low-concentration limit ($k_0 = 1/\tau_0$), for which the phosphorescence quantum yield is that given above plus a concentration-dependent quenching term (k_q) according to

TABLE 2: Decay Times, τ, at Low Dye Concentrations and Fitted Concentration Quenching Constants, k_q, and Zero-Concentration Decay Times, τ_0, for Z1, Z3, and Pt1 in THF Solution[a]

sample	τ (μs)	k_q (10^7 M^{-1} s^{-1})	τ_0 (μs)	$\bar{\tau}$ (μs)
Z1	0.6			52
Z3	310	7	315	86
Pt1	190	1	198	66

[a] Average decay times $\bar{\tau}$ from a double-exponential model is given for PMMA glasses with a 50 mM dye concentration.

$$k = k_0 + k_q c \leftrightarrow \frac{\tau_0}{\tau} = 1 + k_q \tau_0 c \qquad (2)$$

where c is the chromophore concentration (or molarity), which is assumed to be much greater than the concentration of molecules in the excited state. This equation is known as the Stern−Volmer equation.[29] The ratios of the decay times versus the concentration are plotted in Figure 4B, with a linear fitting of the data. From the curves, we obtain the fitted parameters, which are presented in Table 2. Both quenching processes are found to be diffusion limited, as expected.

Interestingly, the quenching rate is quite different for Pt1 and Z3. Therefore, the exchange mechanism responsible for the quenching process is sensitive to molecular structure, probably in terms of the electron distribution of the excited triplet state. We note that Z3, with the highest quenching rate of ~7 times that of Pt1, has many lone-pair orbitals at the azide groups on the ligands, which may affect the probability of external interaction and the rate of triplet state quenching.

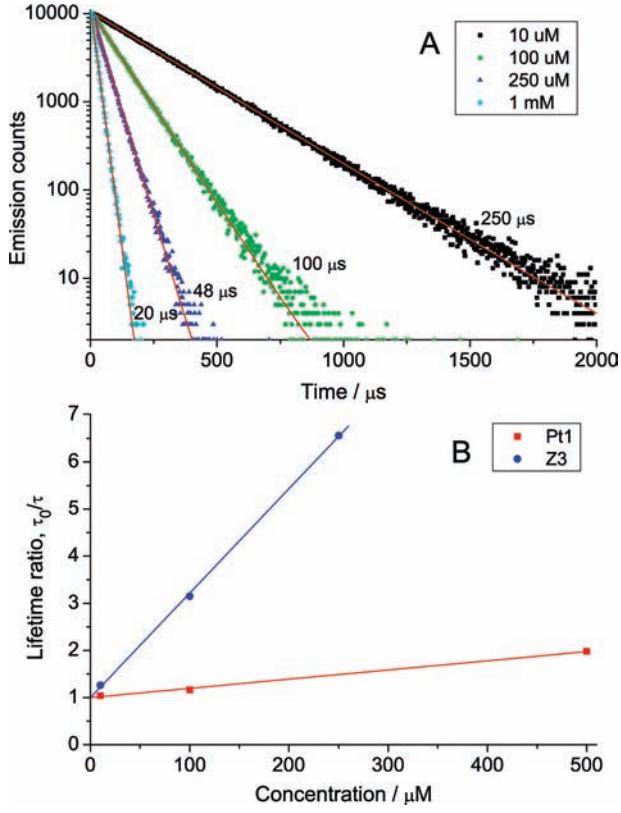

Figure 4. (A) Phosphorescence decay traces of Z3 and (B) phosphorescence decay rates of Z3 and Pt1 measured in THF solution at varying dye concentrations. The decay emission counts were measured at 540 and 525 nm for Z3 and Pt1, respectively, using excitation pulses at 360 nm.

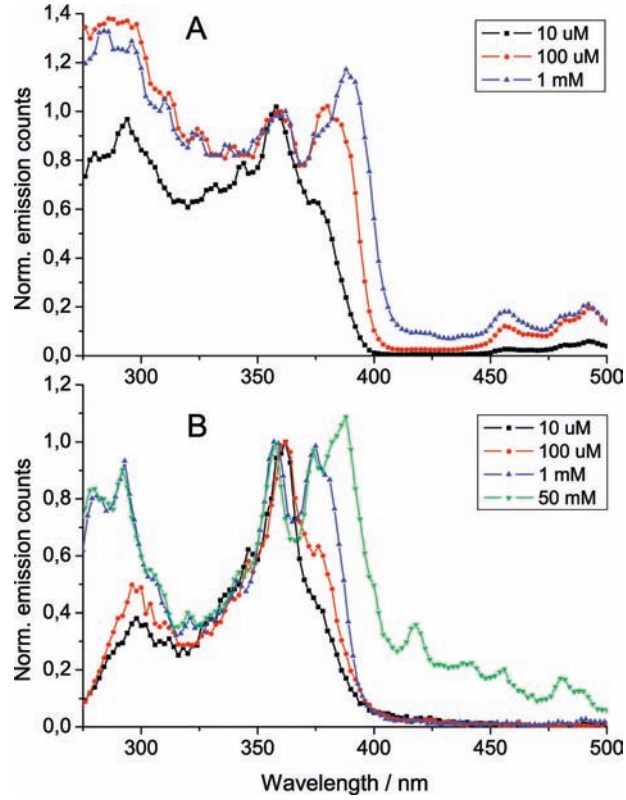

Figure 5. Excitation spectra of Pt1 in (A) THF solution and (B) type I PMMA glass for emission recorded at 525 nm at different concentrations. All spectra are normalized to the 360 nm $S_0 \rightarrow S_1$ absorption peak.

Excitation Spectra. The excitation spectra of Pt1 in Figure 5 were measured when monitoring the emission at the peak of the phosphorescence spectrum at 525 nm, either in an oxygen evacuated THF solution or in a solid PMMA glass. Upon excitation at a specific photon wavelength, the molecular system will return to the ground state via various relaxation channels; the intersystem crossing in Pt1 is efficient (>90%), so most excited molecules relax via channels from the triplet manifold, out of which we detect those that end with phosphorescence of photons around 525 nm (~5%). The spectra in Figure 5 are normalized to have the maximum photon count, which occurs at a wavelength corresponding to the previously discussed $S_0 \rightarrow S_1$ transition, set to unity.

At low concentrations (≤10 μM), the measured excitation spectrum resembles absorption with a single dominant peak around 360 nm with a weak right shoulder and a broad left shoulder that stretches further into the UV region, as shown in Figure 5A. As the chromophore concentration is increased, the right shoulder of the spectrum is enhanced, and another excitation band at 380−390 nm appears. The same behavior was also found for the chromophores embedded in solid PMMA, as shown for Pt1 in type I glass in Figure 5B. Essentially the same behavior was found for all PMMA samples (data not shown). The new excitation feature at 380−390 nm in Figure 5 is clearly a concentration effect, and it can be seen as a splitting of the main peak that occurs at concentrations larger than ~100 μM. The molecular length of the Pt1 molecule is close to 50 Å, so a rotating chromophore of this kind occupies the space of a sphere with radius 25 Å, which corresponds to a (body-centered) cubic close-packed concentration of 17 mM. With chromophore concentrations in the range of 1 to 50 mM, it may thus be reasonable to expect intermolecular electronic

interactions. In a situation of overlapping and interacting electron densities, we can rationalize the observed splittings as a result of a general quantum mechanical splitting that occurs for any two interacting systems (e.g., the formation of bonding and antibonding orbitals in chemistry), leading to an excitation path of lower photon energy for the coupled system. In this context, it would be interesting to pursue a theoretical study of aggregation by means of molecular dynamics, which, however, is beyond the scope of the present work.

Further evidence of the argument of interacting chromophores at high concentrations is seen in the excitation spectra at long wavelengths (425−500 nm). The same characteristic concentration behavior as that shown for Pt1 was also found for Z3 in both solution and PMMA, but the corresponding data have been left out. In this region of the spectra, we expect only nonrelativistically spin-forbidden transitions, which, at low concentrations, cannot be seen on the scale of the spin-allowed transitions. At larger concentrations, however, the relative intensity of transitions in the spin-forbidden region increase substantially, and, at a concentration of 50 mM, we can even see a structure in the spectrum. We interpret this structure to be a resolution of individual triplet states. So why are spin-forbidden transitions more likely to occur at high concentrations? Our explanation would again be that of interacting quantum mechanical systems for which the total angular momentum of two $J = 1$ systems would be a system with $J = \{0, 1, 2\}$, and we would thus be observing transitions from the ground state to the excited state with $J = 0$ of the interacting system.

Transient Excited Triplet State Absorption. The transient absorption spectrum of Z1, Z3, and Pt1 in 10 μM THF solution was measured with a sample thickness of 10 mm. Results are shown in Figure 6A. Because of the fast and efficient intersystem crossing to the triplet state on the order of some picoseconds, the absorption above 400 nm is associated with absorption only from the triplet states. The absorption coefficients at maximum triplet state absorption in the visible region were found to be (1.5, 4.7, and 2.9) $\times$ 10^4 M^{-1} cm^{-1} for Z1, Z3, and Pt1, respectively.[17] The Z1 chromophore show a quite low and noisy signal due to the relatively fast triplet relaxation time compared with the delay time between pump and probe light, as discussed in previous sections.

The corresponding transient absorption spectra of the chromophores in PMMA glasses were also measured at different concentrations. The spectra of Pt1 in type I PMMA glass at concentrations from 10 μM to 50 mM are shown in Figure 6B. We observe a strong and broad triplet absorption just as in the liquid state. The triplet absorption spectrum for Z1, Z3, Pt1, and Pt1−methacrylate in PMMA at 1 mM concentration (100 μM for Z3/PMMA) is depicted in Figure 6C. Because of the much shorter light paths through the 1.5 mm samples compared with the liquid samples, the signals are comparably lower and more noisy. All transient spectra in PMMA glass resemble those found in solution. A red shift of the absorption band of Z1 compared with that of Z3 is found, which is opposite to the corresponding blue shifts observed in the ground-state absorption and phosphorescence emission. This feature was also previously reported comparing other Pt1−acetylides in solution.[17]

In addressing ESA in the triplet manifold from calculations, the choice of molecular structure becomes an issue. We have chosen to adopt the excited-state optimized structures, and the corresponding results are presented in the two right-most columns of Table 1. In this presentation, we have selected the dominating state in the visible region. In typical, the excited-state linear absorption spectra are not dominated by a single

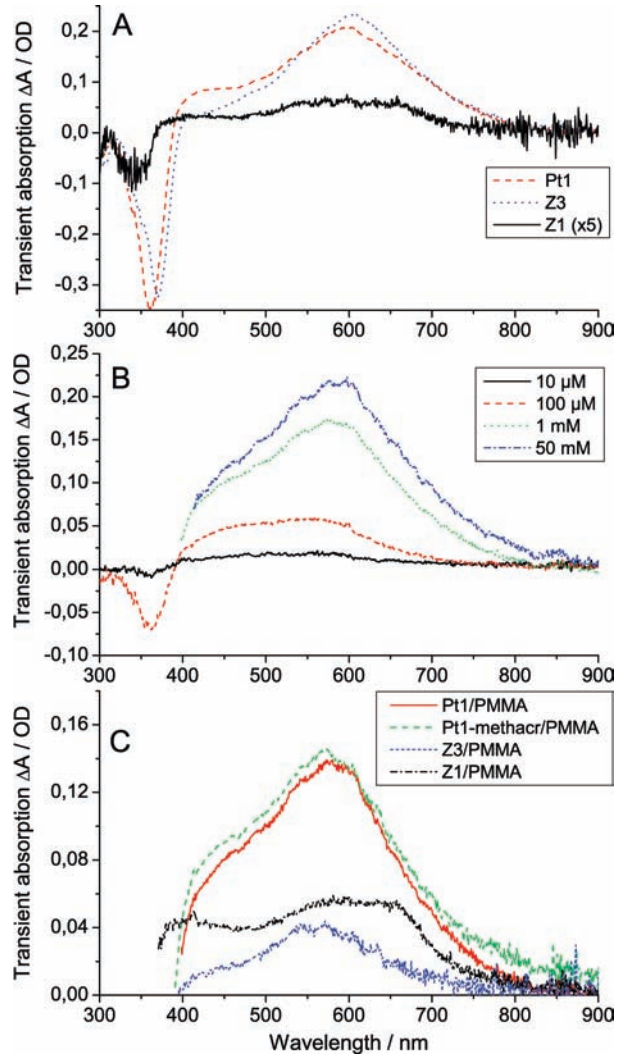

Figure 6. Transient absorption spectra of Z1, Z3, and Pt1. (A) In THF solution at 10 μM dye concentration. (B) Pt1 at four different concentrations in 1.5 mm thick PMMA glasses (type I). (C) In type I and type II PMMA glass at 1 mM concentration (100 μM for Z3).

electronic transition, at least not to the extent that is observed in the corresponding ground-state spectra. For the set of molecules studied here, the ESA is strongest in the region between 450 to 470 nm, and the integrated cross sections of compounds Z1 and Z3 are significantly larger than that of Pt1. The red shift of the Z1 triplet-state absorption, compared with that of Z3, is also supported by the calculations.

Conclusions

In comparison with the liquid state, the basic photophysical properties of platinum(II) acetylides are found to be maintained in solid poly(methyl methacrylate) (PMMA) glasses. At high concentrations, the excitation spectra, measured at the phosphorescence emission channel, show additional low UV-energy bands that are not visible in the low-concentration samples. This is explained by intermolecular electronic interactions and quantum mechanical splitting due to the short distance between adjacent molecules at high concentration. An increased probability for direct triplet excitation in the 400−500 nm region also occurs at high concentrations. Both of these characteristics are observed both in solid-state PMMA and in THF solution. Phosphorescence decay in solution is found to be quenched at higher concentrations. The same is not observed

in solid-state PMMA because of more immobilized chromophores in the solid state. In the comparison of the photophysical properties between type I (dispersed) and type II (covalently bonded) PMMA glasses, no particular differences could be found.

Acknowledgment. This work has been supported by the "Swedish Defence Nano Technology Programme" managed by the Swedish Defence Research Agency (FOI) and the Defence Material Administration (FMV). We thank Dr. Robert Westlund at the Royal Institute of Technology (KTH), Sweden, for providing the chromophores and the solid PMMA materials. P.N. acknowledges financial support from the Swedish Research Council (grant no. 621-2007-5269).

References and Notes

(1) Slusher, R. E. *Rev. Mod. Phys.* **1999**, *71*, S471.
(2) Spangler, C. W. *J. Mater. Chem.* **1999**, *9*, 2013–2020.
(3) Miller, M. J.; Mott, A. G.; Ketchel, B. P. *Proc. SPIE* **1998**, *3472*, 24–29.
(4) Prasad, P. N.; Williams, D. J. *Introduction to Nonlinear Optical Effects in Molecules and Polymers*; Wiley: New York, 1991.
(5) Hollins, R. C. *Curr. Opin. Solid State Mater. Sci.* **1999**, *4*, 189–196.
(6) Tutt, L. W.; Boggess, T. F. *Prog. Quant. Electron.* **1993**, *17*, 299–338.
(7) Baev, A.; Norman, P.; Henriksson, J.; Ågren, H. *J. Phys. Chem. B* **2006**, *110*, 20912–20916.
(8) Staromlynska, J.; McKay, T. J.; Wilson, P. *J. Appl. Phys.* **2000**, *88*, 1726–1732.
(9) Glusac, K.; Köse, M. E.; Jiang, H.; Schanze, K. S. *J. Phys. Chem. B* **2007**, *111*, 929–940.
(10) Rogers, J. E.; Cooper, T. M.; Fleitz, P. A.; Glass, D. J.; McLean, D. G. *J. Phys. Chem. A* **2002**, *106*, 10108–10115.
(11) Lindgren, M.; Minaev, B.; Glimsdal, E.; Vestberg, R.; Westlund, R.; Malmström, E. *J. Lumin.* **2007**, *124*, 302–310.
(12) Staromlynska, J.; McKay, T. J.; Bolger, J. A.; Davy, J. R. *J. Opt. Soc. Am. B* **1998**, *15*, 1731–1736.
(13) Westlund, R.; Glimsdal, E.; Lindgren, M.; Vestberg, R.; Hawker, C.; Lopes, C.; Malmström, E. *J. Mater. Chem.* **2008**, *18*, 166–175.
(14) Westlund, R.; Malmström, E.; Lopes, C.; Öhgren, J.; Rodgers, T.; Saito, Y.; Kawata, S.; Glimsdal, E.; Lindgren, M. *Adv. Funct. Mater.* **2008**, *18*, 1939–1948.
(15) Norman, P.; Ruud, K. Chapter 1: Microscopic Theory of Nonlinear Optics. In *Nonlinear Optical Properties of Matter: From Molecules to Condensed Phases*; Papadopoulos, M. G., Sadlej, A. J., Leszczynski, J., Eds.; Springer: New York, 2006.
(16) Glimsdal, E.; Carlsson, M.; Eliasson, B.; Minaev, B.; Lindgren, M. *J. Phys. Chem. A* **2007**, *111*, 244–250.
(17) Glimsdal, E.; Dragland, I.; Carlsson, M.; Eliasson, B.; Melø, T. B.; Lindgren, M. *J. Phys. Chem. A* **2009**, *113*, 3311–3320.
(18) Bergner, A.; Dolg, M.; Kuchle, W.; Stoll, H.; Preuss, H. *Mol. Phys.* **1993**, *80*, 1431.
(19) Andrae, D.; Haussermann, U.; Dolg, M.; Stoll, H.; Preuss, H. *Theor. Chim. Acta* **1990**, *77*, 123.
(20) Becke, A. D. *J. Chem. Phys.* **1993**, *98*, 5648.
(21) Hehre, W. J.; Ditchfield, R.; Pople, J. A. *J. Chem. Phys.* **1972**, *56*, 2257.
(22) Yanai, T.; Tew, D. P.; Handy, N. C. *Chem. Phys. Lett.* **2004**, *393*, 51.
(23) Peach, M. J. G.; Helgaker, T.; Salek, P.; Keal, T. W.; Lutnæs, O. B.; Tozer, D. J.; Handy, N. C. *Phys. Chem. Chem. Phys.* **2006**, *8*, 558.
(24) Dunning, T. H., Jr. *J. Chem. Phys.* **1989**, *90*, 1007.
(25) Frisch, M. J.; Trucks, G. W.; Schlegel, H. B.; Scuseria, G. E.; Robb, M. A.; Cheeseman, J. R.; Montgomery, J. A.; Jr.; Vreven, T.; Kudin, K. N.; Burant, J. C.; Millam, J. M.; Iyengar, S. S.; Tomasi, J.; Barone, V.; Mennucci, B.; Cossi, M.; Scalmani, G.; Rega, N.; Petersson, G. A.; Nakatsuji, H.; Hada, M.; Ehara, M.; Toyota, K.; Fukuda, R.; Hasegawa, J.; Ishida, M.; Nakajima, T.; Honda, Y.; Kitao, O.; Nakai, H.; Klene, M.; Li, X.; Knox, J. E.; Hratchian, H. P.; Cross, J. B.; Adamo, C.; Jaramillo, J.; Gomperts, R.; Stratmann, R. E.; Yazyev, O.; Austin, A. J.; Cammi, R.; Pomelli, C.; Ochterski, J. W.; Ayala, P. Y.; Morokuma, K.; Voth, G. A.; Salvador, P.; Dannenberg, J. J.; Zakrzewski, V. G.; Dapprich, S.; Daniels, A. D.; Strain, M. C.; Farkas, O.; Malick, D. K.; Rabuck, A. D.; Raghavachari, K.; Foresman, J. B.; Ortiz, J. V.; Cui, Q.; Baboul, A. G.; Clifford, S.; Cioslowski, J.; Stefanov, B. B.; Liu, G.; Liashenko, A.; Piskorz, P.; Komaromi, I.; Martin, R. L.; Fox, D. J.; Keith, T.; Al-Laham, M. A.; Peng, C. Y.; Nanayakkara, A.; Challacombe, M.; Gill, P. M. W.; Johnson, B.; Chen, W.; Wong, M. W.; Gonzalez, C.; Pople, J. A. *Gaussian 03*, revision B05; Gaussian, Inc.: Pittsburgh, PA, 2003.
(26) *DALTON*, a molecular electronic structure program, release 2.0, 2005. http://www.kjemi.uio.no/software/dalton/dalton.html.
(27) Paterson, M. J.; Christiansen, O.; Pawlowski, F.; Jørgensen, P.; Hättig, C.; Helgaker, T.; Salek, P. *J. Chem. Phys.* **2006**, *124*, 054322.
(28) Glimsdal, E.; Carlsson, M.; Eliasson, B.; Lindgren, M. *Proc. SPIE* **2007**, *6740*, 67400M.
(29) Lakowicz, J. R. *Principles of Fluorescence Spectroscopy*, 2nd ed.; Kluwer Academic/Plenum Publishers: New York, 1999.
(30) Slagle, J. E.; Cooper, T. M.; Krein, D. M.; Rogers, J. E.; McLean, D. G.; Urbas, A. M. *Chem. Phys. Lett.* **2007**, *447*, 65–68.

JP905437C